STRONG GROUND MOTION IN NORMAL-FAULTING EARTHQUAKES: OBSERVATIONS AND THEIR IMPLICATIONS FOR EARTHQUAKE HAZARD ASSESSMENT AND EARTHQUAKE SOURCE PROCESSES

R. Westaway[1]

ABSTRACT

Normal-faulting earthquakes occur in regions of active extension, which include parts of western North America, the Aegean Sea region in the eastern Mediterranean, Italy, China, and New Zealand. The relative sparseness of ground acceleration data for normal-faulting earthquakes and the widespread observation that active normal faults are segmented, such that a large earthquake may involve rupture of several fault segments in succession rather than a single fault, both cause difficulties in the quantification of ground acceleration in normal-faulting earthquakes. Some previous studies have suggested that a normal-faulting earthquake of a given size may be expected to produce much smaller ground acceleration than an earthquake of equivalent size with another focal mechanism type. This has led to suggestions that structures in regions where normal-faulting earthquakes of a given size are expected need not be designed to such stringent standards as those where earthquakes of equivalent size but with other focal mechanism types are expected. However, the available ground acceleration values observed in a worldwide set of normal-faulting earthquakes overall differ negligibly, if at all, from those expected for other earthquakes. This implies that one does not need to derive separate equations for predicting ground acceleration in normal-faulting earthquakes: the existing equations that have been derived for other earthquake types are adequate.

INTRODUCTION

Normal-faulting earthquakes occur in numerous regions worldwide that are actively-extending. However, because regions with relatively dense installations of accelerograph stations, such as parts of Japan and coastal parts of California, experience other types of earthquake, the set of ground acceleration data available for normal-faulting earthquakes is relatively limited. Despite this limitation, it is of clear importance to determine whether or not the strength of ground shaking, expressed as peak horizontal ground acceleration or PHGA, is typically the same for normal-faulting earthquakes as for other events. The first part of this article summarises previous work on this subject. Although some differences between some normal-faulting and other

[1] Lecturer (Assistant Professor), Department of Geological Sciences, 4University of Durham, South Road, Durham DH1 3LE, England.

earthquakes have previously been suggested, it appears that if the available ground acceleration data set for normal-faulting earthquakes is examined as a whole, PHGA values are typically not significantly different from those expected for other earthquakes. Length restrictions require this summary to be brief, but most of this material is already published in full elsewhere. The second part examines in much greater detail the extensive PHGA data set available for the 1980 Campania-Basilicata normal-faulting earthquake in southern Italy, which is remarkable both for its complexity and because some records of it appear to show PHGA much larger than, and others show PHGA much smaller than, the values expected. Factors that contribute to these discrepancies are investigated in detail.

COMPARISON OF PEAK HORIZONTAL GROUND ACCELERATION FOR NORMAL-FAULTING AND OTHER EARTHQUAKES

Normal-faulting earthquakes occur in regions where the earth's crust is extending, for example in parts of the western United States and northwestern Mexico, Italy, the high Andes, the Aegean Sea, the margins of the Red Sea, Tibet and southern China, and northern New Zealand. Typically, only the uppermost ~10 km of the earth's crust is at sufficiently low temperature (<~300 °C for brittle deformation processes, such as slip on faults, to occur: at greater depths and higher temperatures the crust deforms plastically. Fault rupture in relatively large earthquakes typically initiates near the base of this brittle layer, propagating predominantly upward and horizontally. Many studies have established that normal faults are segmented, although the typical length of segments appears to differ from region to region, being up to ~20 km in the Aegean region and up to ~50 km in parts of the western USA [1] [2]. Although the demonstrable ability to isolate parts of a fault zone with independent rupture histories constitutes the principal basis for subdividing any major normal fault into segments, examples exist (such as the 1980 Campania-Basilicata earthquake in southern Italy) where rupture on one fault segment appears to trigger fault rupture on an adjacent segment. The result may be a complex earthquake that involves multiple fault ruptures.

The size of an earthquake can be quantified by various parameters, including its surface-wave magnitude M_S, body-wave magnitude m_b, local magnitude M_L, and seismic moment M_O. Each type of magnitude is a logarithmic measure of the amplitude of a particular type of seismic wave. Seismic moment provides instead a measure of the total elastic strain energy that is released in an earthquake. For slip on a rectangular fault plane with along-strike length L and downdip length H, it can be defined as

$$M_0 = \mu \, u \, L \, H \qquad (1)$$

where u is the average slip and μ is the shear modulus of the rocks surrounding the fault (typically ~3×10^{10} Pa). A further logarithmic measure of earthquake size, moment-magnitude or M_w, can be derived from seismic moment. A definition of M_w [3] such that

$$\log_{10} (Mo / Nm) = 1.5 \, M_w + 9.05 \qquad (2)$$

gives M_W values that approximate to M_S for earthquakes in the magnitude range ~5-7.

TABLE 1. Normal-faulting earthquakes with $M_s > 5$ for which ground acceleration records are available

Date	Time	M_s	M_o (10^{18} Nm)	N	Name
1935 Oct 31	18:37	(6.0)	(1)	1	Helena, Montana
1935 Nov 28	14:41	(5.8)	(0.6)	1	Helena, Montana
1935 Nov 28	14:42	(5.8)	(0.6)	1	Helena, Montana
1959 Aug 18	06:37	7.5	100	2	Hebgen Lake, Montana
1962 Aug 30	13.35	5.7	0.3	1	Cache Valley, Utah
1975 Aug 1	20:20	5.7	(0.4)	5	Oroville, California
1976 Aug 19	01:12	(5.0)	(0.04)	1	Denizli, Turkey
1977 Dec 16	07:37	(5.0)	(0.04)	1	Izmir, Turkey
1978 Jun 20	20:03	6.4	(4)	1	Thessaloniki, Greece
1979 Jul 18	13:12	(5.0)	(0.04)	1	Dursunbey, Turkey
1979 Sep 19	21:35	5.5	(0.2)	5	Norcia, Italy
1980 Nov 23	18:34	6.8	(20)	21	Campania, Italy
1980 Nov 23	18:35	(6.3)	3	12	Campania, Italy
1981 Feb 24	20:53	6.7	11	1	Corinth, Greece
1981 Feb 25	02:35	6.4	4	1	Corinth, Greece
1983 Jul 5	12:01	5.8	1.6	5	Biga, Turkey
1983 Oct 28	14:06	7.3	30	6	Borah Peak, Idaho
1983 Oct 29	23:29	(5.0)	0 2	3	Borah Peak, Idaho
1983 Oct,29	23:39	(5.0)	(0.04)	3	Borah Peak, Idaho
1984 Apr 29	05:02	5.2	0.3	5	Gubbio, Italy
1984 May 7	17:49	5.8	0.6	15	Abruzzo, Italy
1984 May 11	10:41	5.2	0.2	12	Abruzzo, Italy
1986 Sep 13	17:24	5.9	(0.8)	1	Kalamata, Greece
1987 Mar 2	01:35	5.2	(0.07)	1	Edgecumbe, New Zealand
1987 Mar 2	01:42	6.6	10	3	Edgecumbe, New Zealand
1987 Mar 2	01:51	5.6	(0.3)	1	Edgecumbe, New Zealand

The higher the ratio of u to the dimensions L and H of the fault, the greater the strain released by the earthquake, and hence the greater the stress drop for a given shear modulus. For normal-faulting earthquakes u is typically $<\sim 10^{-4}$ L. With the above shear modulus, this suggests that average coseismic stress drop for normal-faulting earthquakes is limited to ~3 MPa or ~30 bar. Theoretical models of seismic radiation from faults suggest that the strength of this radiation, which may be expressed quantitatively as the peak horizontal ground acceleration (PHGA), increases with stress drop.

Strike-slip faults and reverse faults do not appear to exhibit the same marked scales of segmentation as normal faults, and it is unclear **a priori** whether or not coseismic stress drop is typically the same as for normal faults. Some people have suggested by indirect reasoning that normal-faulting earthquakes show larger stress drops than other events [4]. If so, one would expect this to be evident from direct comparison of PHGA values also. Some previous work has

indicated that this is the case [5], although the comparison was made using limited amounts of data from restricted localities. A necessary first step in any such comparison is therefore to collect as much PHGA data as possible for normal-faulting earthquakes. The data collected by Westaway and Smith [6] for earthquakes with M_S 5 or greater are listed in Table 1, in which N denotes the number of sets of ground acceleration records available for each earthquake.

Two well-established equations for predicting PHGA are by Joyner and Boore [7] and Campbell [8]; both were derived using data primarily from reverse-faulting and strike-slip earthquakes. Joyner and Boore suggested that:

$$A_J / ms^{-2} = 0.937 \exp (0.573\, MS_W) \exp (-0.00587\, (R / km)) / R \qquad (3)$$

where

$$R^2 = D^2 + k^2 \qquad (4),$$

D being the distance between the recording station and the closest point on the surface projection of the fault and k being an empirical constant equal to 7.3 km. A_J is a prediction for the greatest acceleration observed on either horizontal component record.

In contrast, Campbell [8] proposed an empirical equation of form

$$A_C / m\,s^{-2} = 0.156 \exp (0.868\, M) [R + h \exp (0.7\, M)]^{-1.09} \qquad (5).$$

A_C is a prediction for the mean of the maximum values of ground acceleration on the two horizontal components. Here, M is M_S for earthquakes with M_S above 6, and M_L for smaller events, and h is an empirically-determined constant equal to 0.0606 km. R is the distance between the recording station and the closest point on the fault rupture. Near the earthquake source, both equations predict similar, and roughly constant, values of PHGA. At greater distances, predicted PHGA tails off more rapidly in the case of the Joyner and Boore equation. However, these two equations for predicting PHGA use different definitions of magnitude, source-station distance and PHGA. Comparisons with observations must take these differences of definition into account. The search for possible magnitude-dependent and/or distance-dependent differences between PHGA for normal-faulting and other earthquakes is facilitated by use of the Joyner and Boore equation, which has separable magnitude-dependence and distance-dependence of PHGA. In contrast, Campbell's equation assumes that the form of the decay of PHGA with distance is magnitude dependent. Partly for this reason and partly because of length restrictions, detailed comparison with observed PHGA in this article is restricted to the Joyner and Boore equation.

It is evident that any set of PHGA data shows considerable scatter, both for a given earthquake and between earthquakes. For example, the individual data used by Joyner and Boore [7] give ratios of observed to predicted PHGA between 0.1 and 4. Some of this difference may arise because the different earthquakes considered had different stress drops. However, given the

extent of this scatter, it may be expected to be difficult to resolve any systematic difference between PHGA for normal-faulting and other earthquakes, even if this expected difference is as large as a factor of 3 as has previously been argued [5]. Nonetheless, if a magnitude ~7 reverse-faulting or strike-slip earthquake typically causes PHGA ~2 m s^{-2} at ~20 km distance [7], it is clearly of some relevence to form a view as to whether a magnitude ~7 normal-faulting earthquake at the same distance is expected to cause PHGA ~2 m s^{-2}, ~0.6 m s^{-2}, or some intermediate value.

Westaway and Smith [6] carried out the appropriate comparisons between PHGA observations for normal-faulting earthquakes and PHGA predicted using both equations (3) and (5). They found that overall the observations match the predictions, indicating that PHGA at a given distance from a normal-faulting earthquake of a given size is typically the same as for a reverse-faulting or strike-slip event. However, like in Joyner and Boore's compilation of PHGA data, some observations of PHGA for normal-faulting earthquakes were much larger than expected, but others were much smaller than expected. Readers are referred to this publication [6] for details of this comparison.

PEAK HORIZONTAL GROUND ACCELERATION FOR THE 1980 CAMPANIA-BASILICATA EARTHQUAKE

The 1980 Campania-Basilicata earthquake in southern Italy was one of the largest (M_S 6.8, M_O ~26×10^{18} Nm [9]) normal-faulting events this century. Many people have studied it in detail (see [9], [10], [11]), with the result that it is overall probably the best-documented normal-faulting earthquake of its size to date. It is noted for the substantial data set of ground acceleration observations (Table 1) which, although from a much smaller number of stations than would be typically recorded for a major reverse-faulting or strike-slip earthquake in a densely-instrumented region such as California, is nonetheless the most extensive for any normal-faulting earthquake to date.

This earthquake primarily involved a sequence of ruptures of normal faults with northwesterly strike and ~60° dip to the northeast, with along-strike extent at least 35 km and vertical extent between the earth's surface and ~10-12 km depth (Figures 1 and 2). According to a recent re-investigation of this earthquake [11], fault rupture most likely initiated at or near the SE end of the Carpineta fault segment. Rupture propagated northwestward along this segment (1), and then along the adjacent Marzano segment (2), apparently without interruption. Rupture on the Picentini segment (3) followed. At some stage, possibly at about the same time as the Carpineta rupture, a separate rupture propagated southeastward away from roughly the same place along the San Gregorio fault segment (5). The existence of all four of these ruptures is supported by surface faulting; they occurred in crystalline limestone basement rock, which preserves fault scarps well. An additional NW-propagating rupture (4) possibly occurred on the Castelfranci fault segment, northwest of the Picentini segment. No surface faulting has been identified at this locality, but this may be because this rupture was too small to reach the earth's surface. Alternatively, surface faulting may have occurred during the earthquake, but, given the local soft

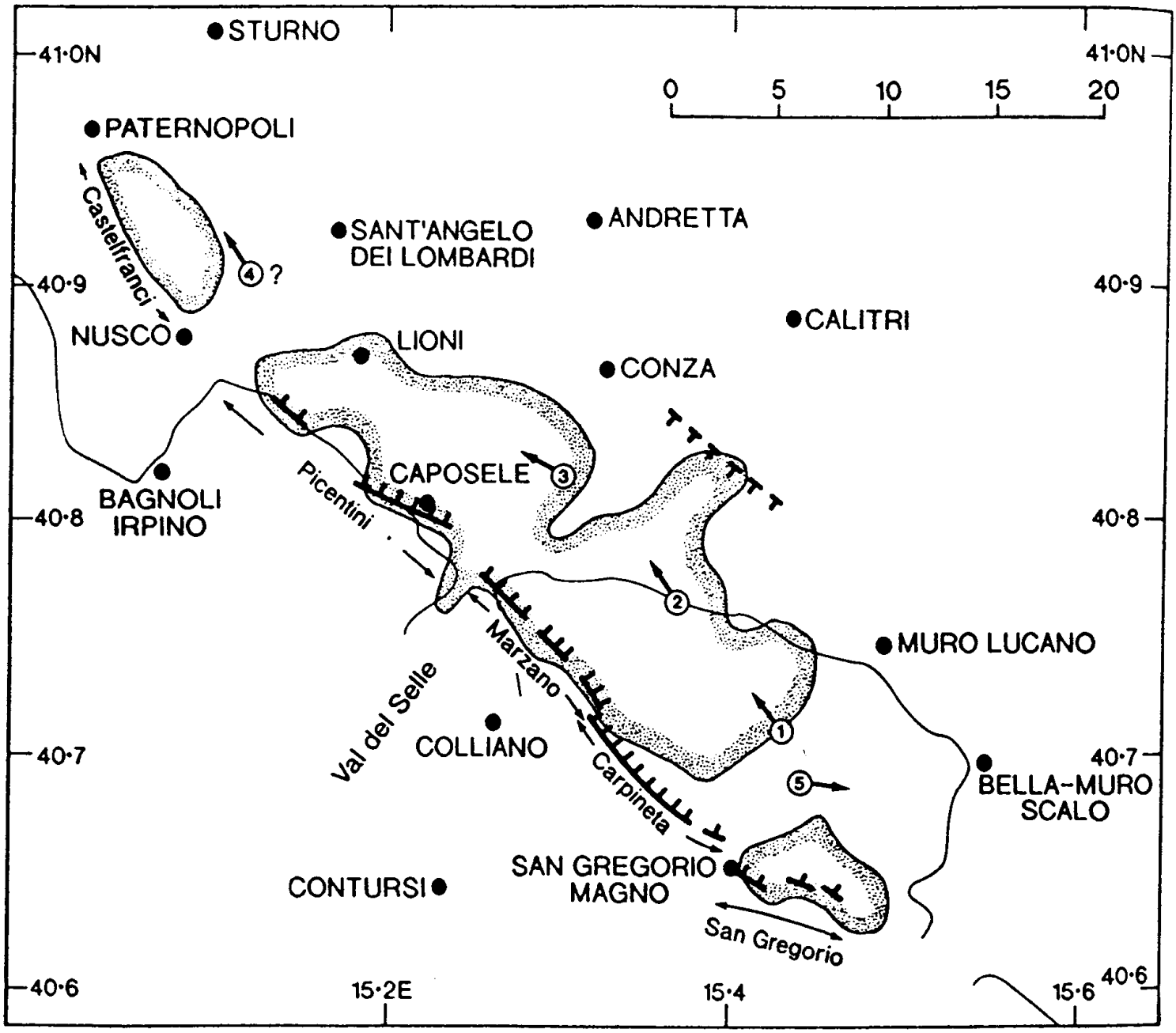

FIGURE 1. Summary map of the epicentral area of the 1980 Campania-Basilicata earthquake. Thick lines indicate observed surface faulting (from [9], [10], [11]), with hanging-wall ticks. Dashed thick line indicates the possible position of the surface trace of fault that slipped in the 40 s aftershock. Thin line indicates northeastern margin of Mesozoic crystalline limestone outcrop, within which faults are relatively well-exposed. Speckled shading outlines the most concentrated aftershock activity. Numbers indicate individual fault ruptures, described in more detail in Table 2. The Castelfranci fault rupture is not proven by association with surface faulting, but seems likely given the local aftershock concentration.

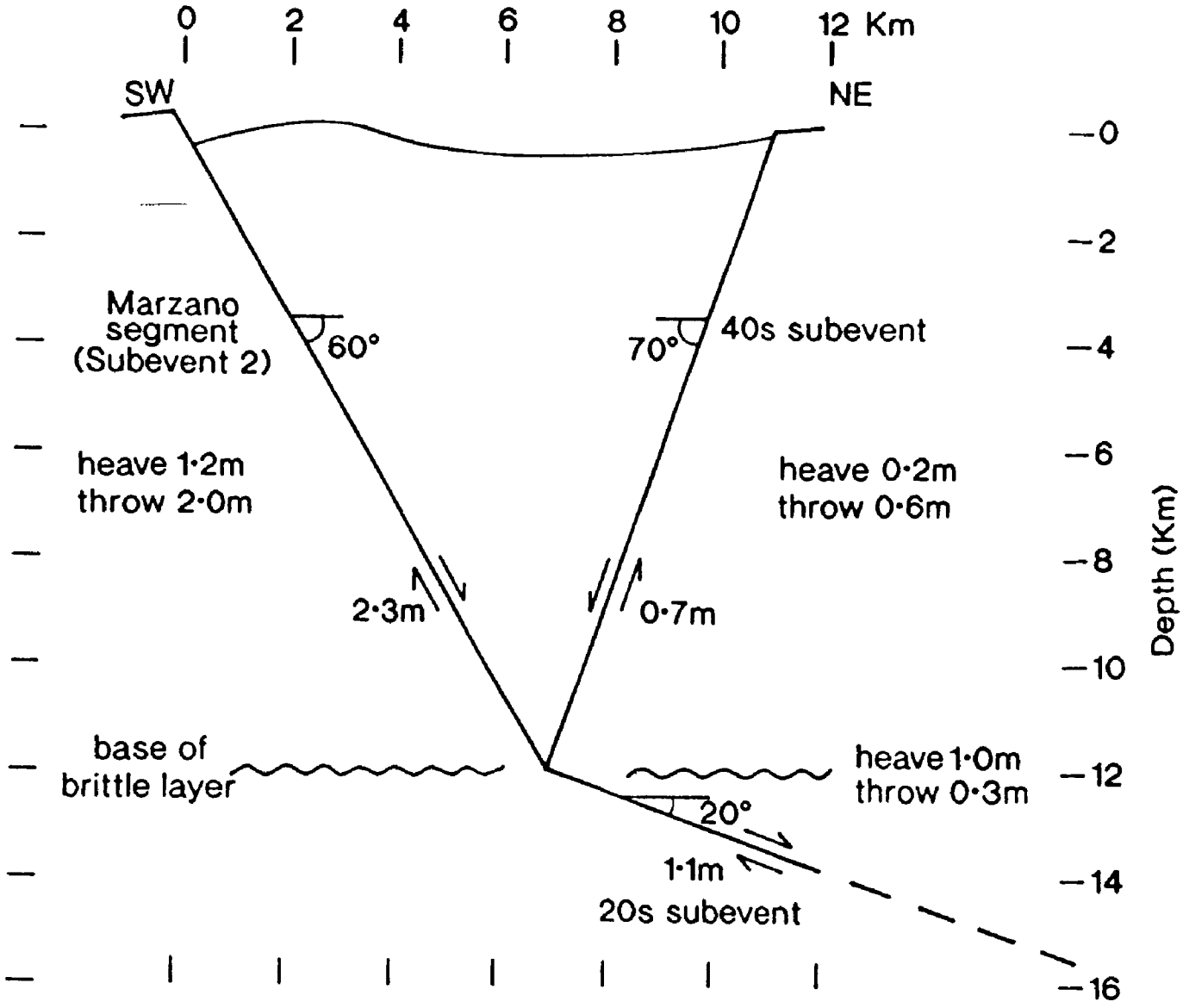

FIGURE 2. Southwest-northeast cross-section across the Marzano segment of surface faulting in Figure 1, indicating schematically the apparent relationship between faults with different orientations that slipped at different times in the 1980 Campania-Basilicata earthquake.

sediments, may have been rapidly obliterated by weathering. The principal evidence in support of the Castelfranci rupture (apart from the character of strong motion records at one station, Sturno, near it) is the local existence of a dense cluster of aftershocks. All other aftershock clusters of equivalent density were associated with faulting in the mainshock (Figure 1). Seismic moment of the Castelfranci rupture is estimated assuming it involved displacement to length ratio 10^{-4}, with its along-strike extent equal to that of the local aftershock cluster.

TABLE 2: Seismic moment release on individual normal faults in the 1980 Campania-Basilicata earthquake

Number+Name	L (km)	u_z (m)	M_O(F) (10^{18} Nm)	M_O(S) (10^{18} Nm)	ϕ (°)	ψ	t (s)	M_w
1 Ruptures on faults dipping northeast at ~60°								
1. Carpineta	9	0.5	2.4	2.5	315	NW	0	6.2
2. Marzano	10	1.0	6.7	6.2	315	NW	2.5	6.5
3. Picentini	14	0.6	4.5	4.5	300	NW	6.8	6.4
(4. Castelfranci	~8	~0.5	~2.2	~2.0	330	NW	~12.8?	6.2)
5. San Gregorio	7	0.5	1.9	(2.0)	300	SE	~0?	6.2
TOTAL	40-48		15.5-17.7	15.2-17.2				
2. Rupture dipping northeast at 20° at base of brittle layer								
20 s subevent				4.0	315	NE	~19	6.4
3. Rupture on fault dipping southwest at ~70°								
40 s subevent				3.0	135	?	~38	6.3
TOTAL				22.2-24.2				

The ~4-5 fault ruptures that occurred within ~10 s on steep, northeast-dipping faults were followed after ~20 s by an apparent low-angle rupture at the base of the brittle layer, which was followed in turn after ~40 s by an apparent rupture on a steep SW-dipping normal fault that reaches the earth's surface ~11 km NE of the NE-dipping faults [10], [11]. The geometrical relationship between the various faults that are known or inferred to have slipped is summarised in Figure 1 and Table 2. In Table 2, L is along-strike length; u_z is vertical slip, observed or estimated, at the earth's surface; M_O (F) and M_O (S) are field and seismological estimates for seismic moment; ϕ is strike; ψ y is rupture direction; and t is the estimated nucleation time after the initial rupture initiated. M_O (F) is estimated using equation (1); M_O (S) is estimated from teleseismic waveform modelling.

Westaway and Smith [6] compiled observations of PHGA for both the mainshock and the 40 s aftershock (Table 3), and attempted to compare these with predicted values. A_N^{max} A_E^{max} and A_H^{max} are peak accelerations on the north-south, and east-west component records, and the peak of the horizontal two-component vector sum. Coordinates of the accelerograph stations that recorded these PHGA values are listed in Table 4. Two immediate problems made comparison of observed and predicted PHGA difficult for the mainshock. First, the spatial extent of its source was unclear, and, second, the magnitude that should be used in the comparison was also unclear. The overall seismic moment of ~26×10^{18} Nm corresponds using equation (2) to M_w 6.91. However, only ~$15.2\text{-}17.2\times10^{18}$ Nm of seismic moment appears to be associated with ruptures on steep NE-dipping faults that ruptured in the early part of the earthquake, corresponding to M_w 6.75-6.79. Even this smaller amount of seismic moment was released in several fault ruptures, and

the individual rupture that actually generated the PHGA will thus have been even smaller. M_0 for the aftershock has been estimated by teleseismic waveform modelling as $3x10^{18}$ Nm [9], corresponding to M_w ~6.3. However, the timing of this aftershock led to interference between its waveforms and those of other seismic phases radiated by the mainshock, and the reliability of this estimate is thus difficult to judge. Westaway and Smith [6] also noted that observed PHGA for this aftershock was substantially less than is expected for an event with M_w ~6.3.

TABLE 3. Observed peak horizontal ground acceleration in the 1980 Campania- Basilicata earthquake

Station	A_N^{max} (m s^{-2})	A_E^{max}(m s^{-2})	A_H^{max} (m s^{-2})
	(i) mainshock		
AU	0.438	0.449	0.541
AZ	0.283	0.334	0.359
BC	0.868	0.803	0.946
BE	0.385	0.567	0.567
BI	1.145	1.533	1.542
BO	0.363	0.372	0.375
BZ	2.179	1.651	2.200
CL	1.101	1 153	1.357
GA	0.369	0.325	0.406
MS	0 879	1.132	1.237
RV	0.665	0.633	0.712
SS	0.261	0.217	0.261
TC	0.470	0.370	0.522
TG	0.586	0.415	0.586
VI	0.369	0.348	0.373
	(ii) 40 s aftershock		
AU	0.160	0.177	0.242
BC	0.581	0.654	0.834
BE	0.132	0.110	0.144
BI	0.450	0.345	0.455
BO	0.213	0.209	0.232
BZ	0.372	0.379	0.413
CL	1.462	1.458	1.895
MS	0.372	0.409	0.538
RV	0.724	0.724	0.965
ST	0.538	0.657	0.710
TC	0.263	0.243	0.268
TG	0.181	0 212	0.235

TABLE 4 Accelerograph station coordinates for the 1980 Campania-Basilicata earthquake

Station	Lautude	Longitude	Name
AU	40°33.62'	15°33.50	Auletta
AZ	41°01.72'	14°28.00	Arienzo
BC	41°00.78'	15°32.55	Bisaccia
BE	41°07.28'	14°47.73	Benevento
BI	40°40.25'	15°04.17'	Bagnoli Irpino
BO	41°15.03'	15°30.58'	Bovino
BZ	40°28.45'	15°30.58'	Brienza
CL	40°55.02'	15°26.32'	Calitri
GA	41°15.53'	13°49.60'	Garigliano
MS	40°47.48'	14°45.85'	Mercato San Severino
RV	40°55.77	15°40.18'	Rionero in Vulture
SS	41°41.03'	15°23.17'	San Severo
ST	41°01.35'	15°07 03'	Sturno
TC	40°37.25'	16°09 42'	Tricarico
TG	40°48.07'	14°23 13'	Torre del Greco
VI	41°52.72'	16°09.87'	Vieste

In the future, many of these problems may be able to be addressed by modelling the ground acceleration records. Some attempts have already been made to do this (e.g., [12], [13]), but they are made difficult by relatively complex structure of the region and the typical need to filter observed seismograms to a range of frequency (usually at relatively low frequency) that available techniques can synthesize. Most such studies require rupture on the Castelfranci fault segment to explain the character of the records at Sturno. However, in some cases modelling of the ground

acceleration records has attempted to constrain parameters such as the dip and strike of other fault segments that are well-constrained independently and has led to estimates that differ from those that are actually observed. However, the extent to which this has caused estimates of other source parameters to be incorrect is unclear.

TABLE 5: Comparison of observed and predicted peak horizontal ground acceleration at localities in the epicentral area of the 1980 Campania-Basilicata earthquake

Station	a_j / ms^{-2}	Segment	M_w	D / km	R / km	A_j / ms^{-2}	a_j / A_j
CL	1.153	2	6.5	12	14	2.255	0.45
BI	1.533	3	6.4	6	9	3.693	0.42
		2	6.5	15	17	2.068	0.74
ST	2.565	4	6.2	5	9	3 530	0.73
		3	6.4	13	15	2.256	1.14
		2	6 5	27	28	1.177	2.18

The problems of identifying the actual fault rupture that generated the observed PHGA are most critical for the three closest accelerograph stations (Calitri, Bagnoli Irpino and Sturno), which are much nearer some fault segments than others (Table 5). For Calitri, the Marzano fault rupture was not only the largest, but also the closest, and thus seems most likely to have been the source of the PHGA. However, this leads to observed PHGA being only 45% of what is expected. The Picentini rupture was much closer than any other to Bagnoli Irpino, but this leads to observed PHGA being only 42% of what is expected. If one assumes that PHGA at Bagnoli Irpino was caused by the more distant, but larger, Marzano rupture, observed PHGA is still only ~74% of what is expected. Problems are most acute for Sturno. It is evident that if the Marzano rupture was assumed to cause the observed PHGA, observed PHGA is much greater than is expected [9]. If the Picentini rupture caused the observed PHGA, it is slightly greater than expected. If, however, the Castelfranci rupture caused the observed PHGA, as seems likely on other grounds (see above), it is only 73% of what is expected. It thus appears that observed PHGA was substantially less than is expected at all stations in the epicentral area.

TABLE 6: General comparison of observed and predicted peak horizontal ground acceleration for the 1980 Campania-Basilicata mainshock

Station	D / km	R / km	a_j / ms^{-2}	A_j / ms^{-2}	a_j / A_j
ST (4)	5	9	2.565	3.530	0.73
BI (3)	6	9	1.533	3.693	0.42
CL (2)	12	14	1.153	2.555	0.45
AU	25	26	0.449	1 282	0.35
BC	29	30	0.868	1.090	0.80
RV	30	31	0.665	1 044	0.64
BZ	32	33	2.179	0.970	2.25
MS	41	42	1.132	0.723	1.57
BO	52	53	0.372	0.537	0.69
BE	53	54	0.567	0.524	1.08
TC	67	67	0.470	0.391	1.20
AZ	72	72	0.334	0.356	0.94
TG	73	73	0.586	0.347	1.69
SS	97	97	0.261	0.227	1.15
GA	132	132	0.369	0.136	2.71
VI	138	138	0.369	0.125	2.95

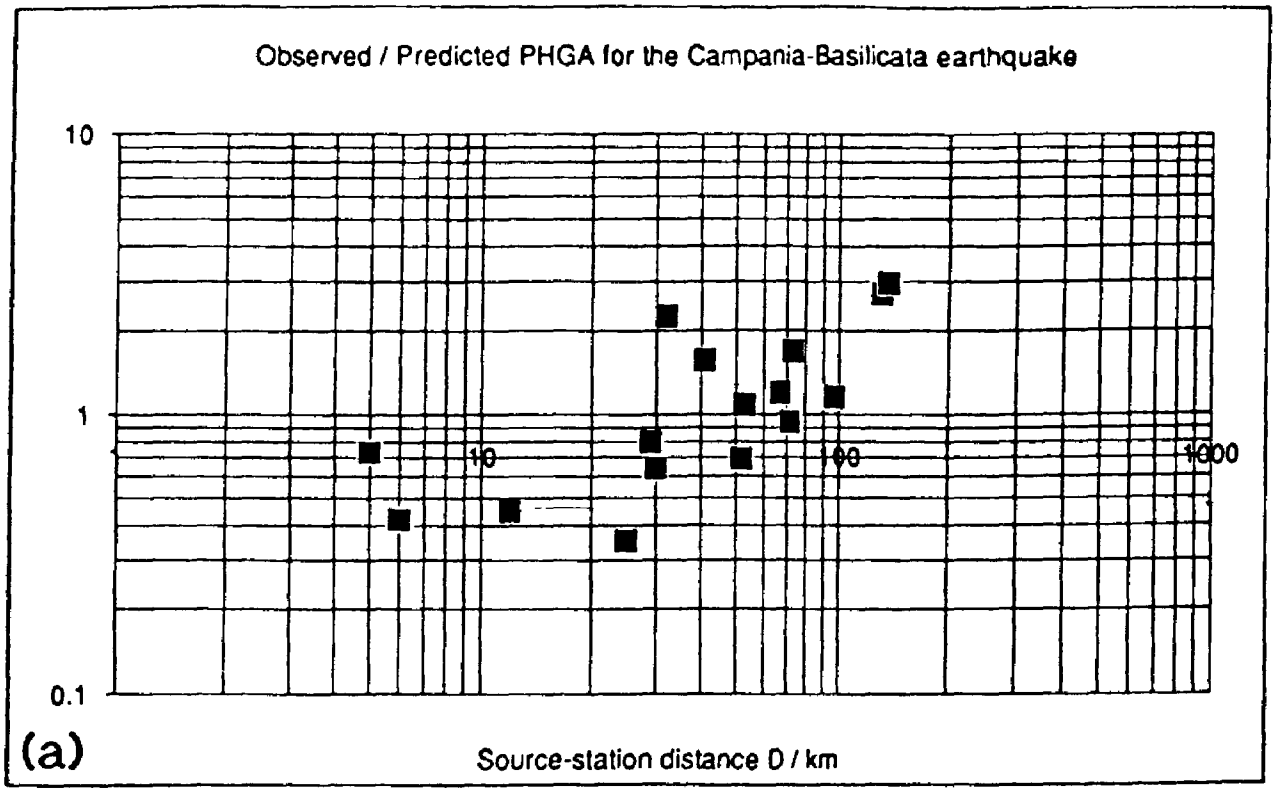

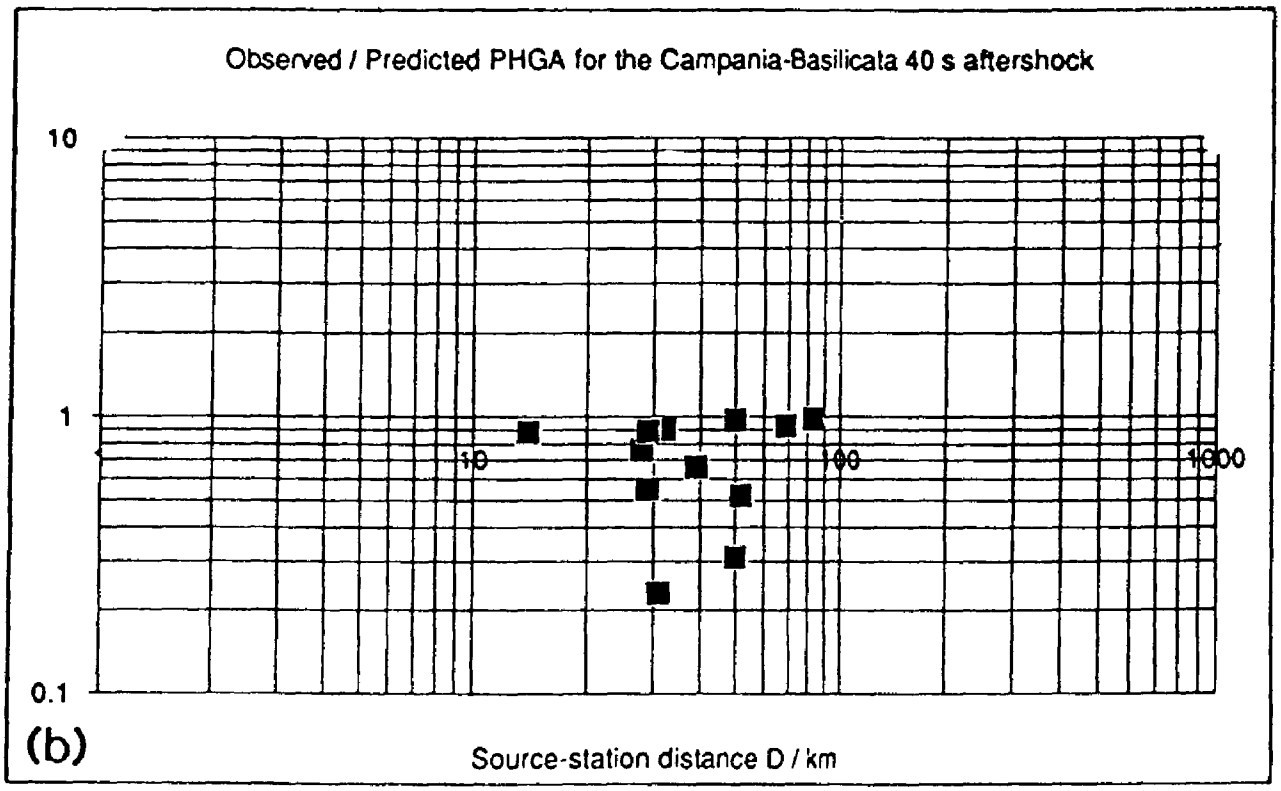

FIGURE 3. Comparison of the ratio of observed to predicted PHGA for the Joyner and Boore equation, summarizing the data from Tables 6 and 7, (a) for the Campania-Basilicata mainshock and (b) for its 40 s aftershock. In (a), observed PHGA is typically overestimated near the source and underestimated farther away. Reasons for this are discussed in the text. In (b), observed PHGA is always overestimated. This may be because this event was of lower magnitude than has been previously thought.

For more distant stations, which are less sensitive to the detailed fault rupture pattern, it is reasonable to assume that the largest, Marzano, rupture caused the observed PHGA. Table 6 compares observed and predicted PHGA on this basis. For simplicity, the Marzano rupture has been assumed centred on latitude 40° 46'N, longitude 15°19'E, and to have involved average horizontal extent 10 km. Distances of each station from this point have been measured, and 5 km has then been subtracted to account approximately for the finite extent of the source, to give the values of D in Table 6. Some of the more distant stations show much larger values of PHGA than are expected, whereas others show smaller values. The two extremes are Auletta, which showed observed PHGA only 35% of what was expected, and Brienza, where it was 2.25 times what was expected. Spectral studies [14] establish that the large PHGA at Brienza was associated with a resonance at ~5-7 Hz frequency. This appears to have been caused by the local site conditions, which comprise shallow alluvial sediments. The instrument at Auletta appears to have triggered late and to have missed most of the main part of the earthquake, which may possibly have generated larger local PHGA than was recorded (see, e.g., [9]). Excluding these two outliers, the data fit a trend in which the ratio of observed to predicted PHGA increases as one moves farther from the earthquake source (Figure 3).

TABLE 7: General comparison of observed and predicted peak horizontal ground acceleration for the 1980 Campania-Basilicata 40 s aftershock

Station	D / km	R / km	a_j / ms^{-2}	A_j / ms^{-2}	a_j / A_j
CL	14	16	1.462	1.659	0.88
BC	28	29	0.654	0.848	0.76
BI	29	30	0.450	0.815	0.55
RV	29	30	0 724	0.815	0.89
AU	31	32	0.177	0.755	0.23
ST	32	33	0.657	0.728	0.90
BZ	39	40	0.379	0.576	0.66
MS	50	51	0.409	0.424	0.97
BE	50	51	0.132	0.424	0.31
BO	52	52	0.213	0.413	0.52
TC	69	69	0.263	0.282	0.93
TG	83	83	0.212	0.216	0.98

Westaway and Smith [6] noted that the Joyner and Boore equation tends to underestimate observed PHGA at distances > ~100 km. It is possible that the typical underestimation observed at distances ~50-100 km may also be a result of the form of this equation, and the apparent overestimation at distances <~20 km may possibly also be an artefact of the form of this equation: it may attempt to compensate for underestimating observed PHGA at greater distances by overestimating it nearer the earthquake source.

Table 7 presents data in the same way as Table 6 but for the 40 s aftershock. Even though predicted PHGA values are calculated for M_W only 6, they remain substantially smaller than are expected. Perhaps this aftershock was even smaller still.

In order to test for this possibility, the set of PHGA data used by Joyner and Boore [7] to derive their prediction equation is considered further. Although they considered data from many earthquakes, the majority of the data used for the earthquake size range comparable to

TABLE 8. Peak horizontal ground acceleration data for stations within 30 km of the San Fernando and Imperial Valley earthquakes

Station	D / km	R / km	a_j / m s^{-2}	A_j / m s^{-2}	a_j / A_j
San Fernando, California, 9 February 1971, M_w 6.6 (reverse-faulting)					
128	17.0	18.5	3.669	1.994	1.84
126	19.6	20.9	1.962	1.741	1.13
127	20.2	21.5	1.442	1.686	0.86
141	21.1	22.3	1.844	1.618	1.14
266	21.9	23.1	2.001	1.555	1.29
125	23.4	24.5	1.491	1.454	1.03
110	24.2	25.3	3.286	1.401	2.34
135	24.6	25.7	2.129	1.376	1.55
475	25.7	26.7	1.118	1.317	0.85
262	28.6	29.5	1.472	1.173	1.26
Imperial Valley, California, 15 October 1979, M_w 6.5 (strike-slip)					
Meloland	0.5	7.3	3.139	5.097	0.62
5028	0.6	7.3	5.101	5.097	1.00
942	1.3	7.4	7.063	5.026	1.41
Aeropuerto	1.4	7.4	3.139	5.026	0.62
5054	2.6	7.7	7.946	4.821	1.65
958	3.8	8.2	6.278	4.514	1.39
5165	5.1	8.9	5.003	4.142	1.21
117	6.2	9.6	3.924	3.824	1.03
955	6.8	10.0	5.984	3.663	1.63
5055	7.5	10.5	2.551	3.478	0.73
County Center	7.6	10.5	2.354	3.478	0.68
Mexicali	8.4	11.1	4.513	3.278	1.38
5060	8.5	11.2	2.158	3.247	0.66
412	8.5	11.2	2.256	3.247	0.69
5053	10.6	12.9	2.747	2.791	0.98
5058	12.6	14.6	3.728	2.442	1.53
5057	12.7	14.6	2.649	2.442	1.08
Cucapah	12.9	14.8	3.041	2.406	1.26
5051	14.0	15.8	1.962	2.240	0.88
Westmoreland	15.0	16.7	1.079	2.109	0.51
5115	16.0	17.6	4.218	1.990	2.12
Chihuahua	17.7	19.1	2.649	1.818	1.46
931	18.0	19.4	1.472	1.787	2.28
5056	22.0	23.2	1.472	1.461	1.01
5059	22.0	23.2	1.472	1.461	1.01
5061	23.0	24.1	1.275	1.399	0.91
Compuertas	23.2	24.3	1.864	1.386	1.34
Cerro Prieto	23.5	24.6	1.668	1.367	1.22
286	26.0	27.0	2.060	1.228	1.68
5062	29.0	29.9	1.275	1.090	1.17

Campania-Basilicata, for stations at distances $<\sim 30$ km, came from two events: San Fernando (reverse-faulting) and Imperial Valley (right-lateral strike-slip). These data are presented in Table 8. For San Fernando, none of the stations used is particularly near the surface projection of the fault plane, and the precise definition of distance is thus not critical. For this earthquake the majority of the observations used are within $\sim$20% of the predictions, but one or two stations show much larger PHGA than is predicted. In contrast, for Imperial Valley some stations show observed PHGA more than double that predicted, whereas others show observed PHGA barely half that predicted. Some of the most dramatic discrepancies between observed and predicted PHGA arise for the nearest stations, situated within $\sim$10 km of the surface projection of the fault plane. Although none shows a ratio of observed to predicted PHGA as low as at Bagnoli Irpino or

Calitri for the 1980 Campania-Basilicata event, differences between observed and predicted PHGA for some stations that recorded the Imperial Valley event are much greater than any observed for Campania-Basilicata. Two factors in particular may contribute to this.

First, the radiation pattern for S-waves may well, to some extent, contribute to the large PHGA values observed near the Imperial Valley fault plane. Points directly above a strike-slip fault rupture lie at a maximum of the S-wave radiation pattern where the S-wave energy is predominantly in the SH-wave component. S-wave amplitude averaged over the whole radiation pattern is typically only ~70% of that at its maxima. If observed PHGA values at stations within 5 km of the Imperial Valley fault rupture are scaled down by a factor of 0.7 to compensate for this effect, all but one (at station 5054) would be less than predicted by Joyner and Boore [7]. Two stations (Meloland and Aeropuerto) would indeed show revised observed PHGA only 43% of that predicted, an overprediction that is more or less as bad as that for Bagnoli Irpino and Calitri. Both Bagnoli Irpino and Calitri in contrast lie near nodal surfaces of the SH-wave radiation pattern for the downdip limit of the fault plane at its closest point (this radiation pattern is displayed in Figure 6 of [9]). The S-wave signal at these stations may thus be expected to be predominantly the SV-wave component. Assuming straight raypaths with 45° plunge, this SV-wave component will be expected to be partitioned equally between vertical and horizontal components of ground acceleration. The maxima of both vertical and horizontal components will thus each be $1/2^{1/2}$ or ~70% of the maximum amplitude of the SV-wave. Furthermore, because the raypath azimuths to these stations from the closest points on the respective fault planes are oriented northeastward and southwestward, the horizontal component of the SV-wave will be expected to be partitioned between these two components of ground motion, with maybe only ~70% of its amplitude on each. This effect may thus potentially result in the maximum amplitude of each individual horizontal component of ground acceleration being only ~50% of the maximum amplitude of the SV-phase.

Second, the parameterization of source-station distance used may also have a critical effect. With the value of h determined as 7.3 km, the definition of source-station distance used is equivalent to saying that the observed PHGA was generated by rupture of a point source at 7.3 km depth below the point on the surface projection of the fault plane that is closest to each station. For a station within a few kilometres of a vertical strike-slip fault, rupture of even a small patch of the fault at shallow depth may well thus cause much larger ground acceleration than is expected. Use of the parameter h effectively limits source station distance to values no less than 7.3 km, and ruptures that are actually closer to stations are thereby represented as though they were more distant. The possibility that some patches of the Imperial Valley fault plane at shallow depth may have ruptured seismically, whereas others at shallow depth may have slipped aseismically (possibly because at these localities the fault plane is lubricated by gouge) may possibly explain the variability between observed values of PHGA at the different stations that are within a few kilometres of different parts of this fault plane. In contrast, this measure of distance does not represent true source-station distances well at the discrepant close stations for the Campania-Basilicata earthquake. At Calitri, where the fault plane dips towards the station, D is ~12 km. However, this distance corresponds to the surface projection of a point at the downdip

limit of the fault plane, at 10-12 km depth, which is thus at least ~16 km [$(12^2 + 10^2)^{1/2}$ km] distant from this station. The observed surface faulting, the updip limit of the fault plane, is ~18 km from Calitri. Increasing the effective source-station distance from ~14 km (the value of R in Table 6) to ~16 km (the minimum actual distance to the fault plane) reduces predicted PHGA from 2.555 m s^{-2} to 2.210 m s^{-2}, and thus increases the ratio of observed to predicted PHGA from 45% to 52%. At Bagnoli Irpino, the 6 km value of D corresponds to the distance to the closest part of the Picentini surface faulting, which dips away from this station. If PHGA at Bagnoli Irpino was generated by rupture of a part of this fault at the base of the brittle layer, actual distance of the station from the closest point above the fault rupture would have been 12 km, and the actual distance to the station from this point on the fault plane would have been at least ~16 km [$(12^2 + 10^2)^{1/2}$ km] also. Aftershocks near the Picentini fault segment are concentrated in the lower part of the brittle layer, indicating that the shallower part of this fault segment may not have ruptured seismically [9]. With source-station distance 16 km instead of 9 km as in Table 6, predicted PHGA would be 2.087 m s^{-2} instead of 3.693 m s^{-2}, and observed PHGA would have thus been ~73% of what was expected, not ~42%.

Both of these factors, the different extent of partitioning of the S-wave signal between the vertical and horizontal components of ground acceleration for stations near strike-slip and dip-slip faults, and the parameterization of source-station distance, thus may well contribute to making observed PHGA appear anomalously small both for the two stations closest to the principal Campania-Basilicata fault ruptures, and for stations near dip-slip faults in general. The ray path orientation in these two cases causes further partitioning of ground acceleration between components of horizontal ground acceleration. The Joyner and Boore [7] definition of PHGA as the maximum of either horizontal component thus also contributes to making observed PHGA appear anomalously small in these cases.

CONCLUSIONS

Overall, the available data indicate that normal-faulting earthquakes generate PHGA that is typically no different from that expected for other sorts of earthquake. However, one widely-used equation for predicting PHGA, by Joyner and Boore [7], appears to underestimate PHGA at large distances but overestimate it for normal-faulting earthquakes when very near the source. This overestimation may result in part from the more complex way in which SH-wave motion is typically partitioned between vertical and horizontal components of ground motion for normal-faulting earthquakes, and in part because of the way in which source-station distance has been measured, which sometimes gives unsatisfactory results for earthquakes on inclined faults. The relatively high PHGA values observed near the strike-slip fault plane that ruptured in the Imperial Valley earthquake may well represent the maxima of the S-wave radiation pattern for this event. A normal-faulting earthquake of the same size would not have the maximum of its S-wave radiation pattern in this position, and may thus not be expected to show such large PHGA values. However, there is no reason to believe that, if averaged over the whole radiation pattern, PHGA is anything other than equal for normal-faulting earthquakes and other types of earthquake of equivalent size.

REFERENCES

1. Roberts, S., and J. Jackson, "Active normal faulting in central Greece: an overview", in "The geometry of normal faults", Geological Society of London special publication 56, edited by A.M. Roberts, G. Yielding, and B. Freeman, pp. 125-142, Blackwell Scientific, Oxford, England, 1991.

2. Machette, M.N., S.F. Personius, A.R. Nelson, D.P. Schwartz, and W.R. Lund, "The Wasatch fault zone, Utah - segmentation and history of Holocene earthquakes", J. Struct. Geol., vol. 13, pp. 137-149, 1991.

3. Hanks, T.C., and H. Kanamori, "A moment magnitude scale", J. Geophys. Res., vol. 84, pp. 2348-2350, 1979.

4. Cocco, M., and A. Rovelli, "Evidence for the variation of stress drop between normal and thrust faulting earthquakes in Italy",J. Geophys. Res., vol. 94, pp. 9399-9416, 1989.

5. McGarr, A., "Scaling of ground motion parameters, state of stress and focal depth", J. Geophys. Res., vol. 89, pp. 6969-6979, 1984.

6. Westaway, R., and R.B. Smith, "Strong ground motion in normal-faulting earthquakes", Geophys. J., vol. 96, pp. 529-559, 1989.

7. Joyner, W.B., and D.M. Boore, "Peak horizontal acceleration and velocity from strong-motion records including records from the 1979 Imperial Valle, California, earthquake, Bull. Seism. Soc. Am., vol. 71, pp. 2011-2038, 1981.

8. Campbell, K.W., Near-source attenuation of peak horizontal acceleration, Bull. Seism. Soc. Am., vol. 71, pp. 2039-2070, 1981.

9. Westaway, R., and Jackson, J., "The earthquake of 1980 November 23 in Campoania-Basilicata, southern Italy", Geophys. J. R. Astr. Soc., 90, 374-443, 1987.

10. Pantosti, D., and G. Valensise, "Faulting mechanism and complexity of the November 23, 1980, Campania-Lucania earthquake, J. Geophys. Res., vol. 95, pp. 15319-15342, 1990.

11. Westaway, R., "Revised hypocentre and fault rupture geometry for the 1980 November 23 Campania-Basilicata earthquake in southern Italy", manuscript in preparation.

12. Siro, L., and C. Chiaruttini, Source complexity of the 1980 southern Italian earthquake from analysis of strong-motion S-wave polarizations", Bull. Seism. Soc. Am., vol. 79, pp. 1810-1832, 1989.

13. Vaccari, F., P. Suhadolc, and G.F. Panza, "Irpinia, Italy, 1980 earthquake: waveform modeling of strong motion data", Geophys. J. Int., vol. 101, pp. 613-647, 1990.

14. Fels, A., A. Pugliese, and F. Muzzi, "Campano-Lucano earthquake, November 1980, Italy: Strong motion data related to local site conditions", Proc. of the annual convention of the Italian national research project on Italian seismicity, Udine, 12-14 May 1991, pp. 105-124, 1991.